

Exact exchange optimized effective potential and self-compression of stabilized jellium clusters

M. Payami

Center for Theoretical Physics and Mathematics,
Atomic Energy Organization of Iran, P. O. Box 11365-8486, Tehran-Iran

(Dated: December 2, 2024)

In this work, we have used the exchange-only optimized effective potential in the self-consistent calculations of the density functional Kohn-Sham equations for simple metal clusters in stabilized jellium model with self-compression. The results for the closed-shell clusters of Al, Li, Na, K, and Cs with $N = 2, 8, 18, 20, 34$, and 40 show that the clusters are 5% more compressed here than in the local spin density approximation.

PACS numbers: 71.15.-m, 71.15.Mb, 71.15.Nc, 71.20.Dg, 71.24.+q, 71.70.Gm

I. INTRODUCTION

The Kohn-Sham (KS)[1] density functional theory (DFT)[2] is one of the most powerful techniques in electronic structure calculations. However, the exact form of the exchange-correlation functional is still unknown and, in practice, one must use approximations. The accuracy of the predictions of the properties depends on how one approximates this functional. The simplest one is the local spin density approximation (LSDA) in which one uses the properties of the uniform electron gas locally [1]. This approximation is in principle appropriate for systems in which the variations of the spin densities n_σ are sufficiently slow. For finite systems and surfaces which are highly inhomogeneous, the generalized gradient approximation (GGA)[3] is more appropriate. In spite of the success of the LSDA and GGA, it is observed that in some cases these approximations fail to predict even qualitatively correct behaviors[4, 5, 6, 7]. On the other hand, appropriate self-interaction corrected versions of these approximations are observed to lead to correct behaviors[7, 8]. These observations motivates one to use functionals in which the self-interaction contribution is removed exactly. One of the functionals, which satisfies this constraint, is the exact exchange (EEX) orbital dependent functional. Using the EEX functional leads to the correct asymptotic behavior of the KS potential as well as to correct results for the high density limit in which the exchange energy is dominated [9]. Although neglecting the correlation effects in orbital dependent functionals fails to reproduce the dispersion forces such as the van der Waals forces[10, 11], the EEX in some respects is advantageous over the local and semi-local approximations[11, 12]. To obtain the local exchange potential from the orbital dependent functional, one should solve the optimized effective potential (OEP) integral equation. Recently, Kümmel and Perdew [13, 14] have invented an iterative method which allows one to solve the OEP integral equation accurately and efficiently even for three dimensional systems. This method is used in this work.

To simplify the cluster problem, one notes that the

properties of alkali metals are dominantly determined by the delocalized valence electrons. In these metals, the Fermi wavelengths of the valence electrons are much larger than the metal lattice constants and the pseudo-potentials of the ions do not significantly affect the electronic structure. This fact allows one to replace the discrete ionic structure by a homogeneous positive charge background which is called jellium model (JM). In its simplest form, one applies the JM to metal clusters by replacing the ions of an N -atom cluster with a sphere of uniform positive charge density and radius $R = (zN)^{1/3}r_s$, where z is the valence of the atom and r_s is the bulk value of the Wigner-Seitz (WS) radius for valence electrons[15, 16, 17]. Assuming the spherical geometry is justified only for closed-shell clusters which is the subject in this work. However, it is a known fact that the JM has some drawbacks[18, 19]. The stabilized jellium model (SJM) in its original form[20] was the first attempt to overcome the deficiencies of the JM and still keeping the simplicity of the JM. Application of the SJM to simple metals and metal clusters has shown significant improvements over the JM results[20]. However, for small metal clusters the surface effects are important and the cluster is self-compressed due to its surface tension. This effect has been successfully taken into account by the SJM which is called SJM with self-compression (SJM-SC)[21, 22]. Application of the LSDA-SJM-SC to neutral metal clusters has shown that the equilibrium r_s values of small clusters are smaller than their bulk counterparts and approaches to it for very large clusters. This trend is consistent with the results of *ab. initio* calculations[23, 24].

In this work we have used the EEX-SJM-SC to obtain the equilibrium sizes and energies of closed-shell neutral N -electron clusters of Al, Li, Na, K, and Cs for $N=2, 8, 18, 20, 34$, and 40 (for Al, $N = 18$ corresponds to Al_6 cluster and other values do not correspond to a real Al_n). Comparison of the results with those in the LSDA-SJM-SC, which also includes correlation, shows that, in the EEX-SJM-SC, the clusters are more compressed. The organization of this paper is as follows. In section II we explain the calculational schemes. Section III is devoted to the results of our calculations and finally, we conclude

this work in section IV.

II. CALCULATIONAL SCHEMES

In this section we first explain how to implement the exact exchange in the SJM, and then will explain the procedure for the OEP calculations.

A. Exact exchange stabilized jellium model

As in the original SJM[20], here the Ashcroft empty core pseudo-potential[25] is used for the interaction of an ion of charge z with an electron at a relative distance r :

$$w(r) = \begin{cases} -2z/r, & (r > r_c) \\ 0, & (r < r_c) \end{cases} \quad (1)$$

The core radius, r_c , will be fixed by setting the pressure of the bulk system equal to zero. In the EEX-SJM, the average energy per valence electron in the bulk with density n is given by

$$\varepsilon(n) = t_s(n) + \varepsilon_x(n) + \bar{w}_R(n, r_c) + \varepsilon_M(n), \quad (2)$$

with

$$t_s(n) = c_k n^{2/3}, \quad (3)$$

$$\varepsilon_x(n) = c_x n^{1/3}, \quad (4)$$

$$c_k = \frac{3}{5} (3\pi^2)^{2/3}, \quad c_x = \frac{3}{2} (3/\pi)^{1/3}. \quad (5)$$

All equations throughout this paper are expressed in Rydberg atomic units. Here t_s and ε_x are the kinetic and exchange energy per particle, respectively. \bar{w}_R is the average value of the repulsive part of the pseudo-potential ($\bar{w}_R = 4\pi n r_c^2$), and ε_M is the average Madelung energy. Demanding zero pressure for the bulk system at equilibrium yields:

$$\{2t_s(n) + \varepsilon_x(n) + 12\pi n r_c^2 + \varepsilon_M(n)\}_{n=n^B} = 0. \quad (6)$$

Solution of this equation for r_c gives

$$r_c(r_s^B) = \frac{(r_s^B)^{3/2}}{3} \{ -2t_s(r_s) - \varepsilon_x(r_s) - \varepsilon_M(r_s) \}_{r_s=r_s^B}^{1/2}. \quad (7)$$

In Fig. 1 we have plotted the core radii for different values of r_s^B which assume 2.07, 3.28, 3.99, 4.96, and 5.63 for Al, Li, Na, K, and Cs, respectively. The result is compared with the case in which the correlation energy is also incorporated [see Eq.(26) of ref.]. As is seen, to stabilize the bulk system in the EEX case, the core radii assume smaller values.

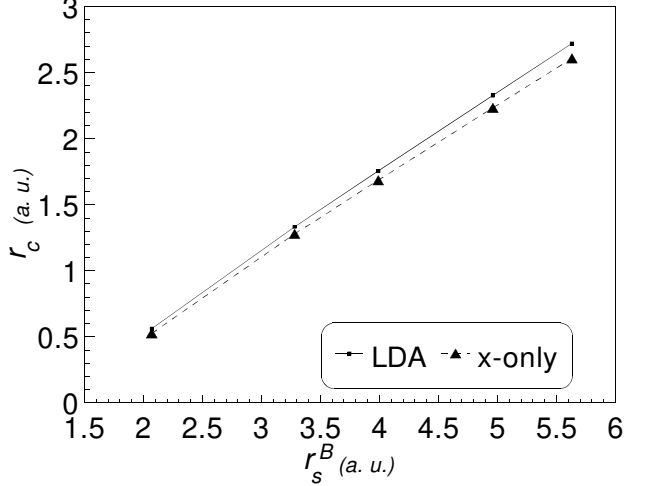


FIG. 1: Pseudo-potential core radii in atomic units for different r_s^B values.

As in the original SJM[20] (but in the absence of the correlation energy component), at equilibrium density we have

$$\langle \delta v \rangle_{WS} = -\frac{1}{3} [2t_s(n^B) + \varepsilon_x(n^B)]. \quad (8)$$

Here, $\langle \delta v \rangle_{WS}$ is the average of the difference potential over the WS cell and the difference potential, δv , is defined as the difference between the pseudo-potential of a lattice of ions and the electrostatic potential of the jellium positive background. Once the values of $\langle \delta v \rangle_{WS}$ and r_c as functions of r_s^B are found, the EEX-SJM total energy of a cluster becomes

$$\begin{aligned} E_{EEX-SJM}[n_\uparrow, n_\downarrow, r_s, r_s^B] &= E_{EEX-JM}[n_\uparrow, n_\downarrow, r_s] \\ &+ (\varepsilon_M + \bar{w}_R) \int d\mathbf{r} n_+(\mathbf{r}) \\ &+ \langle \delta v \rangle_{WS} \int d\mathbf{r} \Theta(\mathbf{r}) [n(\mathbf{r}) - n_+(\mathbf{r})]. \end{aligned} \quad (9)$$

Here,

$$\begin{aligned} E_{EEX-JM}[n_\uparrow, n_\downarrow, r_s] &= T_s[n_\uparrow, n_\downarrow] + E_x[n_\uparrow, n_\downarrow] \\ &+ \frac{1}{2} \int d\mathbf{r} \phi([n, n_+]; \mathbf{r}) [n(\mathbf{r}) - n_+(\mathbf{r})], \end{aligned} \quad (10)$$

$$E_x = \sum_{\sigma=\uparrow, \downarrow} \sum_{i,j=1}^{N_\sigma} \int d\mathbf{r} d\mathbf{r}' \frac{\phi_{i\sigma}^*(\mathbf{r}) \phi_{j\sigma}^*(\mathbf{r}') \phi_{j\sigma}(\mathbf{r}) \phi_{i\sigma}(\mathbf{r}')}{|\mathbf{r} - \mathbf{r}'|}, \quad (11)$$

$$\phi([n, n_+]; \mathbf{r}) = 2 \int d\mathbf{r}' \frac{[n(\mathbf{r}') - n_+(\mathbf{r}')]}{|\mathbf{r} - \mathbf{r}'|}, \quad (12)$$

$$n(\mathbf{r}) = \sum_{\sigma=\uparrow,\downarrow} \sum_{i=1}^{N_{\sigma}} |\phi_{i\sigma}(\mathbf{r})|^2, \quad (13)$$

$$n_+(\mathbf{r}) = n\theta(R-r); \quad n = \frac{3}{4\pi r_s^3}. \quad (14)$$

To obtain the equilibrium size and energy of an N -atom cluster in EEX-SJM-SC, we solve the equation

$$\frac{\partial}{\partial r_s} E(N, r_s, r_c) \Big|_{r_s=\bar{r}_s(N)} = 0, \quad (15)$$

where N and r_c are kept constant and E is given by Eq. (9).

B. The OEP equations

Kümmel and Perdew[14] have proved, in a simple way, that the OEP integral equation is equivalent to

$$\sum_{i=1}^{N_{\sigma}} \psi_{i\sigma}^*(\mathbf{r}) \phi_{i\sigma}(\mathbf{r}) + c.c. = 0. \quad (16)$$

$\phi_{i\sigma}$ are the self-consistent KS orbitals and $\psi_{i\sigma}$ are orbital shifts. The self-consistent orbital shifts and the local exchange potentials are obtained from the iterative solutions of inhomogeneous KS equations. Taking spherical geometry for the jellium background and inserting

$$\phi_{i\sigma}(\mathbf{r}) = \frac{\chi_{i\sigma}(r)}{r} Y_{l_i, m_i}(\Omega), \quad (17)$$

and

$$\psi_{i\sigma}(\mathbf{r}) = \frac{\xi_{i\sigma}(r)}{r} Y_{l_i, m_i}(\Omega), \quad (18)$$

in to the inhomogeneous KS equation (Eq.(21) of Ref.[14]) one obtains[26]

$$\left[\frac{d^2}{dr^2} + \varepsilon_{i\sigma} - v_{eff\sigma}(r) - \frac{l_i(l_i+1)}{r^2} \right] \xi_{i\sigma}(r) = q_{i\sigma}(r). \quad (19)$$

Here, $\varepsilon_{i\sigma}$ are the KS eigenvalues and

$$v_{eff\sigma}(\mathbf{r}) = v(\mathbf{r}) + v_H(\mathbf{r}) + v_{x\sigma}(\mathbf{r}), \quad (20)$$

$$v_H(\mathbf{r}) = 2 \int d\mathbf{r}' \frac{n(\mathbf{r}')}{|\mathbf{r} - \mathbf{r}'|}. \quad (21)$$

The right hand side of Eq. (19) can be written as

$$q_{i\sigma}(r) = q_{i\sigma}^{(1)}(r) + q_{i\sigma}^{(2)}(r), \quad (22)$$

with

$$q_{i\sigma}^{(1)}(r) = [v_{xc\sigma}(r) - \bar{v}_{xc i\sigma} + \bar{u}_{xc i\sigma}] \chi_{i\sigma}(r), \quad (23)$$

and

$$q_{i\sigma}^{(2)}(r) = 2 \sum_{j=1}^{N_{\sigma}} \sum_{l=|l_i-l_j|}^{l_i+l_j} \frac{4\pi}{2l+1} \chi_{j\sigma}(r) B_{\sigma}(i, j, l; r) \times \overline{[I(l_j m_j, l_i m_i, l m_j - m_i)]^2}. \quad (24)$$

The quantities B and I in Eq. (24) are defined as

$$B_{\sigma}(i, j, l; r) = \int_{r'=0}^r dr' \chi_{i\sigma}(r') \chi_{j\sigma}(r') \frac{r'^l}{r'^{l+1}} + \int_{r'=r}^{\infty} dr' \chi_{i\sigma}(r') \chi_{j\sigma}(r') \frac{r^l}{r'^{l+1}} \quad (25)$$

$$I(l_j m_j, l_i m_i, l m) = \int d\Omega Y_{l_j m_j}^*(\Omega) Y_{l_i m_i}(\Omega) Y_{l m}(\Omega), \quad (26)$$

and the bar over I^2 implies average over m_i and m_j . Also, the expression for $\bar{u}_{xi\sigma}$ reduces to

$$\bar{u}_{xi\sigma} = -2 \sum_{j=1}^{N_{\sigma}} \sum_{l=|l_i-l_j|}^{l_i+l_j} \frac{4\pi}{2l+1} \overline{[I(l_j m_j, l_i m_i, l m_j - m_i)]^2} \times \int_0^{\infty} dr \chi_{i\sigma}(r) \chi_{j\sigma}(r) B_{\sigma}(i, j, l; r). \quad (27)$$

The procedure for the self-consistent iterative solutions of the OEP equations is explained in Refs.[14, 26].

In Fig. 2, the self-consistent source terms $q_{i\sigma}(r)$ of Eq. (19) are plotted for the equilibrium size of Na_{18} cluster. The corresponding orbital shifts $\xi_{i\sigma}(r)$ are shown in Fig.3.

III. RESULTS AND DISCUSSION

We have used the EEX-SJM-SC to obtain the equilibrium sizes and energies of closed-shell 2, 8, 18, 20, 34, and 40-electron neutral clusters of Al, Li, Na, K, and Cs.

In Table I we have listed the results for the equilibrium states. As is seen, the equilibrium r_s values of the clusters are almost the same up to 3 decimals for the KLI and OEP schemes whereas, there are significant differences between the OEP and LSDA values. As an example, we have plotted the equilibrium r_s values of the closed-shell K_N clusters in Fig. 4. It shows that the LSDA predicts larger cluster sizes than the KLI and OEP.

To illustrate the trend in the \bar{r}_s values, we plot the difference $(\bar{r}_s^{\text{LSDA}} - \bar{r}_s^{\text{KLI}})$ for all species in Fig. 5. One notes that for a given element, the difference is larger for smaller clusters. On the other hand, the difference for the lower-density element is higher. However, the maximum

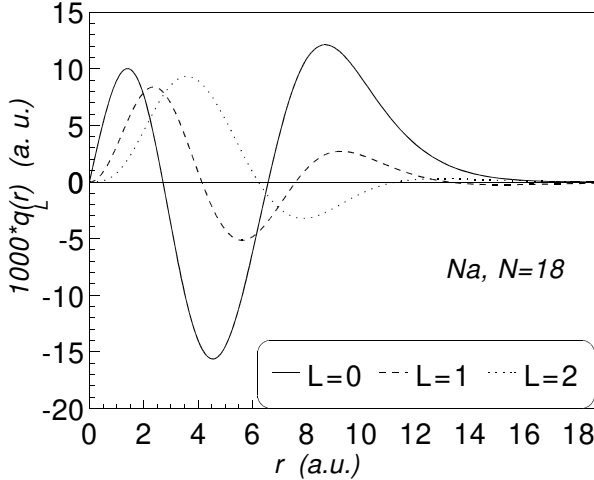


FIG. 2: Right hand side of Eq. (19) for the self-consistent equilibrium size of Na_{18} .

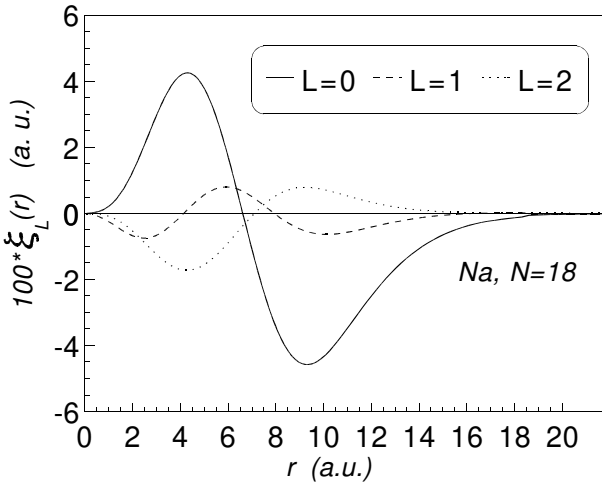


FIG. 3: Orbital shifts in atomic units for the self-consistent equilibrium size of Na_{18} .

relative difference is about 5% which corresponds to the 2-electron cluster of monovalent atom with $r_s^B = 2.07$ (corresponding to Al). We therefore conclude that the EEX-SJM-SC predicts smaller bond lengths, at most 5%, compared to the LSDA-SJM-SC.

Comparison of the equilibrium total energies of the OEP and KLI shows that OEP relative energies are on average 0.009% more negative. This result should be compared to the simple JM results[26] which is 1.2%. We do not compare the total energies of OEP and LSDA because in LSDA there exist a correlation contribution. On the other hand, comparison of the exchange energies show that on the average, the relative exchange energies in OEP is 0.33% more negative than than KLI whereas, it is 11% more negative than the LSDA (it is 9% for the

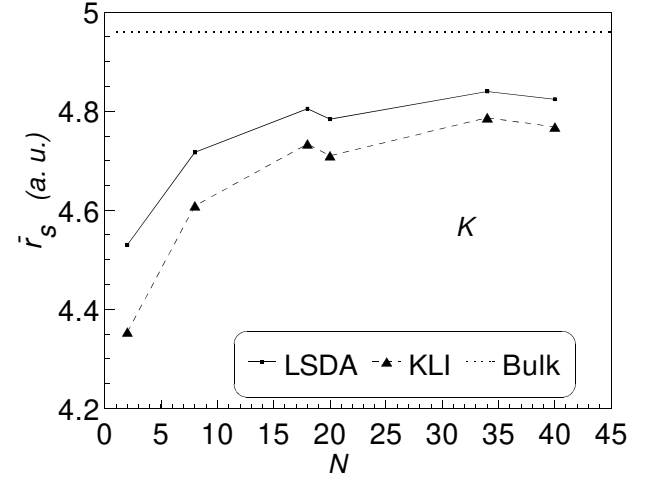


FIG. 4: Equilibrium r_s values of K_N clusters for different sizes. The dotted line is r_s^B . KLI and OEP predict smaller sizes for the clusters.

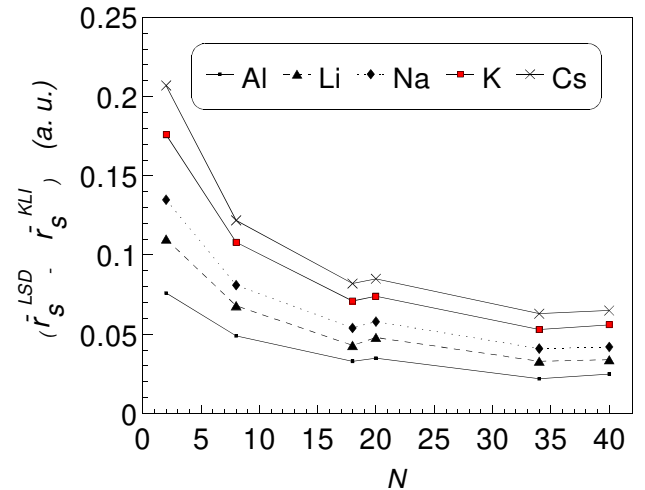


FIG. 5: Difference in the equilibrium r_s values of clusters with different sizes. The difference is larger for lower-density elements.

JM).

As in the simple JM, the OEP KS eigenvalue bands are contracted relative to those of the KLI. That is, for all N , the relation $\Delta^{\text{OEP}} < \Delta^{\text{KLI}}$ holds. Here, $\Delta = \varepsilon_H - \varepsilon_L$ is the difference between the maximum occupied and minimum occupied KS eigenvalues. For the same external potential, the OEP and KLI results coincide for two-electron systems and $\Delta = 0$. The results in TableI show that the maximum relative contraction, $|\Delta^{\text{OEP}} - \Delta^{\text{KLI}}|/\Delta^{\text{KLI}}$, is 2.6% which corresponds to Cs_{18} .

TABLE I: Equilibrium sizes, \bar{r}_s , in bohrs, the absolute values of total and exchange energies as well as highest occupied and lowest occupied Kohn-Sham eigenvalues in rydbergs are compared for KLI, OEP, and LSDA schemes. The LSDA total energies include the correlation energies as well.

Atom	r_s^B	N	\bar{r}_s	KLI				OEP				LSDA					
				$-E_x$	$-\varepsilon_L$	$-\varepsilon_H$	\bar{r}_s	$-E$	$-E_x$	$-\varepsilon_L$	$-\varepsilon_H$	\bar{r}_s	$-E$	$-E_x$	$-\varepsilon_L$	$-\varepsilon_H$	
Al ^a	2.07	2	1.430	1.5700	0.9253	0.8152	0.8152	1.430	1.5700	0.9253	0.8152	0.8152	1.506	1.5585	0.7541	0.5012	0.5012
		8	1.744	5.8640	3.6018	1.1142	0.6714	1.744	5.8647	3.6089	1.1088	0.6713	1.793	6.1204	3.2361	0.8821	0.4605
		18	1.876	12.7709	7.9467	1.1727	0.5507	1.876	12.7734	7.9760	1.1619	0.5492	1.909	13.5947	7.3850	1.0129	0.4009
		20	1.846	14.3309	8.8532	1.1856	0.5000	1.847	14.3319	8.8706	1.1804	0.4993	1.881	15.2718	8.2738	1.0282	0.3622
		34	1.928	23.9914	14.9857	1.2055	0.4826	1.928	23.9968	15.0339	1.1998	0.4789	1.950	25.7679	14.1829	1.0853	0.3649
		40	1.901	28.2841	17.5064	1.2202	0.4490	1.901	28.2863	17.5348	1.2136	0.4450	1.926	30.4900	16.7211	1.0965	0.3401
Li	3.28	2	2.698	1.0076	0.5748	0.4777	0.4777	2.698	1.0076	0.5748	0.4777	0.4777	2.808	1.0264	0.4745	0.2983	0.2983
		8	2.966	3.9138	2.2501	0.5760	0.4157	2.966	3.9144	2.2557	0.5735	0.4158	3.034	4.1678	2.0363	0.4476	0.2937
		18	3.086	8.6776	5.0261	0.5935	0.3601	3.086	8.6798	5.0506	0.5879	0.3591	3.129	9.3963	4.6879	0.5062	0.2738
		20	3.059	9.6670	5.5418	0.5889	0.3221	3.059	9.6682	5.5553	0.5865	0.3228	3.107	10.4905	5.2078	0.5061	0.2423
		34	3.134	16.3774	9.4868	0.6029	0.3282	3.134	16.3823	9.5298	0.5991	0.3258	3.167	17.8728	8.9866	0.5374	0.2620
		40	3.111	19.1876	10.9835	0.5979	0.2971	3.111	19.1898	11.0052	0.5950	0.2960	3.145	21.0418	10.5398	0.5355	0.2366
Na	3.99	2	3.403	0.8409	0.4785	0.3883	0.3883	3.403	0.8409	0.4785	0.3883	0.3883	3.538	0.8646	0.3964	0.2437	0.2437
		8	3.664	3.2841	1.8579	0.4467	0.3406	3.663	3.2846	1.8632	0.4451	0.3408	3.745	3.5261	1.6856	0.3453	0.2434
		18	3.784	7.3064	4.1549	0.4544	0.2989	3.784	7.3084	4.1772	0.4502	0.2981	3.838	7.9710	3.8769	0.3859	0.2308
		20	3.758	8.1240	4.5669	0.4485	0.2672	3.758	8.1251	4.5794	0.4470	0.2682	3.816	8.8856	4.2995	0.3851	0.2042
		34	3.834	13.7980	7.8340	0.4583	0.2750	3.833	13.8028	7.8751	0.4551	0.2730	3.875	15.1665	7.4223	0.4078	0.2236
		40	3.813	16.1410	9.0432	0.4520	0.2480	3.813	16.1431	9.0632	0.4502	0.2477	3.855	17.8365	8.6906	0.4055	0.2017
K	4.96	2	4.354	0.6882	0.3920	0.3100	0.3100	4.354	0.6882	0.3920	0.3100	0.3100	4.530	0.7147	0.3258	0.1957	0.1957
		8	4.609	2.6951	1.5054	0.3408	0.2733	4.609	2.6955	1.5098	0.3396	0.2735	4.717	2.9204	1.3682	0.2622	0.1977
		18	4.734	6.0102	3.3659	0.3416	0.2422	4.734	6.0121	3.3860	0.3385	0.2415	4.805	6.6130	3.1427	0.2894	0.1902
		20	4.710	6.6722	3.6887	0.3356	0.2169	4.710	6.6733	3.7002	0.3349	0.2182	4.784	7.3628	3.4795	0.2885	0.1687
		34	4.787	11.3534	6.3392	0.3419	0.2246	4.787	11.3579	6.3782	0.3393	0.2230	4.840	12.5823	6.0079	0.3042	0.1861
		40	4.768	13.2650	7.2975	0.3355	0.2025	4.768	13.2671	7.3162	0.3346	0.2027	4.824	14.7863	7.0226	0.3023	0.1683
Cs	5.63	2	5.006	0.6123	0.3494	0.2723	0.2723	5.006	0.6123	0.3494	0.2723	0.2723	5.213	0.6395	0.2910	0.1724	0.1724
		8	5.261	2.3990	1.3322	0.2923	0.2405	5.261	2.3994	1.3363	0.2913	0.2406	5.383	2.6135	1.2133	0.2247	0.1752
		18	5.390	5.3547	2.9775	0.2907	0.2141	5.389	5.3564	2.9963	0.2880	0.2134	5.472	5.9215	2.7821	0.2461	0.1696
		20	5.366	5.9403	3.2589	0.2850	0.1921	5.366	5.9414	3.2701	0.2847	0.1935	5.451	6.5894	3.0784	0.2454	0.1509
		34	5.445	10.1156	5.6044	0.2897	0.1992	5.445	10.1200	5.6423	0.2873	0.1977	5.508	11.2652	5.3122	0.2580	0.1668
		40	5.428	11.8123	6.4416	0.2835	0.1797	5.428	11.8144	6.4598	0.2831	0.1801	5.493	13.2347	6.2061	0.2564	0.1512

^aHere, $N=18$ corresponds to Al₆ cluster and other N 's do not correspond to a real Al clusters.

IV. SUMMARY AND CONCLUSION

In this work, we have considered the exchange-only stabilized jellium model in which we have used the exact orbital-dependent exchange functional. This model is applied for the simple metal clusters of Al, Li, Na, K, and Cs. For the local exchange potential in the KS equation, we have solved the OEP integral equation by the iterative method. By finding the minimum energy of an N -atom cluster as a function of r_s , we have obtained the equilibrium sizes and energies of the closed-shell clusters ($N = 2, 8, 18, 20, 34, 40$) for the three schemes of LSD, KLI, and OEP. The results show that in the EEX-SJM,

the clusters are more contracted relative to the ordinary LSDA-SJM, i.e., 5% more contraction. The KLI and OEP results show equal values (up to three decimals) for the equilibrium r_s values.

The total energies in the OEP are more negative than the KLI by 0.009% on the average. It should be mentioned that in the simple JM the KLI and OEP total energies for Al were positive (except for $N = 2$). On the other hand, the exchange energies in the OEP is about 0.33% more negative than that in the KLI whereas, it is about 11% more negative than that in the LSD. The widths of the occupied bands, $\varepsilon_H - \varepsilon_L$ in the OEP are contracted relative to those in the KLI by at most 2.6%.

-
- [1] W. Kohn and L. J. Sham, Phys. Rev. **140**, A1133 (1965).
- [2] P. Hohenberg and W. Kohn, Phys. Rev. **136**, B864 (1964).
- [3] J. P. Perdew, K. Burke, and M. Ernzerhof, Phys. Rev. Lett. **77**, 3865 (1996).
- [4] R. N. Schmid, E. Engel, R. M. Dreizler, P. Blaha, and K. Schwarz, Adv. Quantum Chem. **33**, 209 (1999).
- [5] S. Varga, B. Fricke, M. Hirata, T. Bastug, V. Pershina, and S. Fritzsche, J. Phys. Chem. A **104**, 6495 (2000).
- [6] T. C. Leung, C. T. Chan, and B. N. Harmon, Phys. Rev. B **44**, 2923 (1991).
- [7] P. Dufek, P. Blaha, and K. Schwarz, Phys. Rev. B **50**, 7279 (1994).
- [8] E. Engel and S. H. Vosko, Phys. Rev. B **47**, 13164 (1993).
- [9] J. P. Perdew and S. Kurth, in *Density Functionals: Theory and Applications*, edited by D. P. Joubert, Springer

- Lecture notes in Physics (Springer, Berlin, 1998).
- [10] E. Engel and R. M. Dreizler, *J. Comput. Chem.* **20**, 31 (1999).
 - [11] R. J. Magyar, A. Fleszar, and E. K. U. Gross, *Phys. Rev. B* **69**, 045111 (2004).
 - [12] S. Kümmel, L. Kronik, and J. P. Perdew, *Phys. Rev. Lett.* **93**, 213002 (2004).
 - [13] S. Kümmel and J. P. Perdew, *Phys. Rev. Lett.* **90**, 043004 (2003).
 - [14] S. Kümmel and J. P. Perdew, *Phys. Rev. B* **68**, 035103 (2003).
 - [15] M. Payami, *J. Chem. Phys.* **111**, 8344 (1999).
 - [16] M. Payami, *J. Phys.: Condens. Matter* **13**, 4129 (2001).
 - [17] M. Payami, *Phys. Stat. Sol. (b)* **241**, 1838 (2004).
 - [18] N. D. Lang and W. Kohn, *Phys. Rev. B* **1**, 4555 (1970).
 - [19] N. W. Ashcroft and D. C. Langreth, *Phys. Rev.* **155**, 682 (1967).
 - [20] J. P. Perdew, H. Q. Tran, and E. D. Smith, *Phys. Rev. B* **42**, 11627 (1990).
 - [21] J. P. Perdew, M. Brajczewska, and C. Fiolhais, *Solid State Commun.* **88**, 795 (1993).
 - [22] M. Payami, *Can. J. Phys.* **82**, 239 (2004).
 - [23] U. Röthlisberger and W. Andreoni, *J. Chem. Phys.* **94**, 8129 (1991).
 - [24] M. Payami, *Phys. Stat. Sol. (b)* **225**, 77 (2001).
 - [25] N. W. Ashcroft, *Phys. Lett.* **23**, 48 (1966).
 - [26] M. Payami and T. Mahmoodi, arXiv:physics/0508115.